Role of Charged and Hydrophobic Residues in the Oligomerization of the PYRIN Domain of ASC†

Mie Moriya,§ Shunichiro Taniguchi,§ Peter Wu,‖ Edvards Liepinsh,⊥ Gottfried Otting,‖ and Junji Sagara*,§

Molecular Oncology, Institute on Aging and Adaptation, Shinshu University Graduate School of Medicine, 3-1-1 Asahi, 390-8621, Japan, Research School of Chemistry, Australian National University, Canberra, ACT 0200, Australia, and Department of Medical Biochemistry and Biophysics, Karolinska Institute, S-17177 Stockholm, Sweden

Received July 30, 2004; Revised Manuscript Received October 19, 2004

ABSTRACT: Apoptosis-associated speck-like protein containing a caspase recruitment domain (ASC) is an adaptor protein composed of two homophilic protein−protein interaction domains, a PYRIN domain (PYD) and a caspase recruitment domain. PYD-dependent oligomerization of ASC is thought to play a crucial role in formation of a molecular platform, the inflammasome, which activates caspase-1. When expressed in cells, the PYD of ASC was shown to form cytoplasmic filaments through self-association. Over 70 single point mutants were analyzed for filament formation in cells expressing the mutant proteins. The set of mutations comprised every single amino acid residue with a charged side chain (Arg, Lys, Asp, and Glu) and a large hydrophobic side chain (Ile, Leu, Met, Phe, Pro, and Val). Filament formation of the ASC PYD was prevented by mutation of Lys21, Leu25, Lys26, Pro40, Arg41, Asp48, and Asp51 of helices 2, 3, and 4. These data identify a coherent interaction surface, establishing a molecular model of PYD−PYD complexes with an important role for charge−charge interactions.

We previously identified ASC[1] as a proapoptotic protein containing a caspase recruitment domain (CARD) that formed a large aggregate (called a "speck") in apoptotic cells (*1*). ASC (also termed TMS1 or Pycard) is an adaptor protein composed of two protein−protein interaction domains, an N-terminal PYRIN domain (PYD), and a C-terminal CARD, and has been implicated in apoptosis, inflammation, and cancer (*2*−*7*). The PYD, also called PAAD or DAPIN, is a new member of the six-helix bundle death domain-fold superfamily that includes the death domain (DD), death effector domain (DED), and CARD (*8*). In humans, more than 30 PYD-containing proteins have been identified, including the causative gene products of autoinflammatory diseases, pyrin and cryopyrin (*9*−*11*).

ASC interacts with the proform of caspase-1 via CARD−CARD interactions and stimulates its conversion to its active form (*12*−*15*). The induced proximity model for apoptosis signaling pathways is based on evidence that adaptor protein-induced oligomerization of initiator caspases is essential for their proteolytic activation (*16*, *17*). It is thought that PYD-mediated oligomerization of ASC is a critical prerequisite for assembly of the signal complex activating caspase-1. Therefore, it is important to determine the PYD structure and the critical residues for PYD oligomerization. Recently, the PYD structures of Nalp1 and ASC have been determined by NMR spectroscopy (*18*, *19*). These structures allowed an improved sequence alignment between different PYDs, identifying a number of conserved surface residues that may play a role for a conserved mode of oligomerization. The conservation of PYD surface residues is, however, incomplete, and experimental verification has been missing.

Overexpression of the ASC PYD in cells has been shown to result in filamentous structures in the cytoplasm through self-oligomerization (*4*, *5*). Such cytoplasmic filament-like structures have been observed for many domains of the death domain superfamily (*20*−*23*). For example, overexpression of the DEDs of FADD and caspase-8 results in cytoplasmic filaments, and the CARDs of caspase-2 and mE10 have also been shown to form intracellular filaments through homophilic interactions.

In the present study, we used the generation of filaments to determine the role of each amino acid of the ASC PYD in PYD−PYD interactions. No other assay is currently available that would allow efficient assessment of the activity of a large number of ASC PYD mutants. Seventy-two single point mutants of the charged (Asp, Glu, Arg, and Lys) and hydrophobic (Leu, Ile, Met, Val, Phe, and Pro) residues of the ASC PYD were prepared and analyzed with respect to production of PYD filaments. Combined with the solvent exposure of the respective amino acid side chains in the three-dimensional structure, a continuous surface area with positively and negatively charged residues was identified, which seems to be crucial for oligomerization of the ASC PYD. The data further support the notion that the R42W

† This work was supported in part by the Japan Society for the Promotion of Science (16021218) and the Australian Research Council for a Federation Fellowship (G.O.).

* To whom correspondence should be addressed: Telephone: +81-263-37-2723; Fax: +81-263-37-2724. E-mail: sagara@sch.md.shinshi-u.ac.jp.

§ Shinshu University Graduate School of Medicine.

‖ Australian National University.

⊥ Karolinska Institute.

[1] Abbreviations: ASC, apoptosis-associated speck-like protein containing a CARD; CARD, caspase recruitment domain; DD, death domain; DED, death effector domain; PYRIN domain, pyrin N-terminal homology domain; PYD, PYRIN domain; PAAD, pyrin, AIM2, ASC and death domain-like; DAPIN, domain in apoptosis and interferon response; GFP, green fluorescence protein; NMR, nuclear magnetic resonance.

10.1021/bi048374i CCC: $30.25
Published on Web 12/09/2004

mutation in the pyrin PYD associated with familial Mediterranean fever (FMF) interferes with intermolecular protein−protein interactions.

MATERIALS AND METHODS

Expression Plasmids and Mutations. ASC cDNA encoding the full-length polypeptide (195 residues) was inserted into pcDNA3 (Invitrogen) and pEGFP-c2 (Clontech) as described (*1*, *4*). Constructs encoding GFP-tagged truncated ASC mutants (amino acids 1−100, 1−95, 1−90, and 1−85) were produced by PCR using pEGFP-c2 ASC (amino acids 1−195) as the template (*24*). The primers were designed according to the human ASC mRNA sequence (GenBank Accession No. AB023416). In this study, ASC (amino acids 1−90) is referred to as ASC PYD. A construct encoding C-terminally HA-tagged ASC PYD was produced by PCR using the template plasmid pcDNA3 ASC (amino acids 1−195) and two primers encoding the HA tag sequence (YPYDVPDYA). An N-terminally Flag-tagged ASC PYD construct was made by insertion of the PCR product (amino acids 1−100) into the EcoRI and SalI sites of pFLAG-CMV-4 (Sigma) as described (*4*). Point mutations were introduced into pEGPF-c2 ASC PYD by PCR using primer sets that included the mutations. Mutations in the ASC PYD were confirmed by sequencing. The Expand High-Fidelity system (Roche Molecular Biochemicals) was used for the PCR. The restriction enzymes, T4 polynucleotide kinase, T4 DNA ligase, Klenow Fragment, and M-MLV reverse transcriptase were purchased from Takara Biotechnology (Tokyo, Japan).

Expression and Observation of GFP-Tagged ASC PYD Filaments. Cos7 cells were cultured in Dulbecco's modified minimal essential medium supplemented with 10% fetal bovine serum. One day before transfection, Cos7 cells were seeded on a Lab-Tek 8-chambered coverglass (Nalge Nunc International). A total of 0.1−0.2 μg of pEGFP-c2 ASC PYD and 0.3 μL of the transfection reagent Fugene 6 (Roche Molecular Biochemicals) were mixed and added to cell cultures (0.25 mL of medium) according to the manufacturer's instructions. Fluorescent cells were observed from 12 to 72 h after transfection in the living state using a fluorescent microscope, Axiovert S100 (Carl Zeiss Corporation). Expression levels were measured by Western Blotting as follows. One day before the transfection, Cos7 cells were seeded on 24-well culture plates (Becton Dickinson Labware). A total of 0.3 μg of plasmid DNA and 0.6 μL of Fugene 6 were mixed and added to the cell cultures (0.5 mL of medium) according to the manufacturer's instructions. Twenty-four hours after transfection, the cells were lysed in 0.1 mL of a 1% SDS solution and boiled for 5 min. The cell lysates (20 μg of protein) were electrophoresed in a 10% SDS polyacrylamide gel and electroblotted on a PVDF membrane (Millipore). After the blots were blocked in Tris-buffered saline containing 5% nonfat skim milk, they were incubated with rabbit anti-GFP antiserum (Santa Cruz Biotechnology) and finally detected with the ECL Western blotting detection system (Amersham). The percentage of PYD filament-producing cells was determined by the number of PYD filament-producing cells divided by the total number of fluorescent cells. For each experiment, more than 200 fluorescent cells from randomly chosen fields were counted. The PYD filament-positive mutants usually produced filamentous structures in over 10% of the fluorescent cells, while the negative mutants produced filaments in none or much less than 1% of the fluorescent cells.

Immunostaining. One day before transfection, Cos7 cells were seeded on a coverglass in 30-mm culture dishes. A total of 1 μg of plasmid DNA and 2 μL of Fugene 6 (Roche Molecular Biochemicals) were mixed and added to cell cultures (2 mL of medium). Twenty-four or forty-eight hours after transfection, cells were fixed with 3.7% formaldehyde for 15 min at room temperature. The fixed cells were permeabilized with 0.2% Triton X-100 and then soaked for 15 min with Tris-buffered saline containing 1% bovine serum albumin and 2% fetal bovine serum at room temperature. The filaments of HA- and Flag-tagged ASC PYDs were stained with rabbit anti-HA and anti-Flag antibodies, respectively (Santa Cruz Biotechnology). A rhodamine-conjugated goat anti-rabbit immunoglobulin antibody (Amersham Biosciences) was used as the secondary antibody. Antibodies against tubulin, actin, vimentin, and cytokeratins were purchased from Sigma.

Expression of ASC PYD Mutants in E. coli. The wild-type and a set of mutant ASC PYD genes were inserted into the phage T7 promoter vector pETMCSIII (*25*) between the NdeI and EcoRI restriction sites for subsequent expression with a N-terminal $(His)_6$ tag. The nucleotide sequences were verified using an ABI 3730 sequencer. The proteins were produced in the *Escherichia coli* strain BL21(DE3)/pLysS (*26*). The cells were grown at 37 °C in Luria-Bertani broth containing ampicillin (50 μg/mL) and chloramphenicol (33 μg/mL) and gene expression induced by addition of isopropyl-β-D-thiogalactoside (0.5 mM) when the OD_{595} had reached between 0.5 and 0.8. After further growth for 3 h, the cells were harvested by centrifugation, resuspended in lysis buffer (50 mM Na phosphate at pH 7.7, 300 mM NaCl, 2 mM β-mercaptoethanol) containing spermidine (10 mM), and lysed in a French press. Solubility was determined by comparing the amount of protein in the cell lysate with that in the supernatant fraction on an SDS−PAGE gel. For purification, His_6-tagged soluble recombinant proteins from the supernatants were batch loaded onto Ni-NTA (Qiagen) affinity resins and washed with 20 column volumes of lysis buffer containing 25 mM imidazole, followed by elution in lysis buffer containing 250 mM imidazole.

NMR Measurements. Purified ASC PYD mutants were exchanged into pH 7.2 phosphate buffer (10 mM Na phosphate, 50 mM NaCl, 0.2% NaN_3). D_2O was added to 10% v/v prior to NMR analysis. One-dimensional ^1H NMR spectra were recorded on a Bruker Avance 800 MHz NMR spectrometer at 25 °C.

Solvent Accessibility. Solvent accessibilities of the side chains were calculated with a probe of 1.4 Å radius and compared with the hypothetical accessibility of a fully extended side chain in a helix, where both neighboring residues are Gly (*27*).

RESULTS

PYD Filaments. To determine the minimal segment of ASC required for PYD filament formation, different C-terminal deletion mutants (amino acids 1−100, 1−95, 1−90, and 1−85) of ASC were expressed as fusion proteins with GFP in Cos7 cells. Except for the deletion mutant including

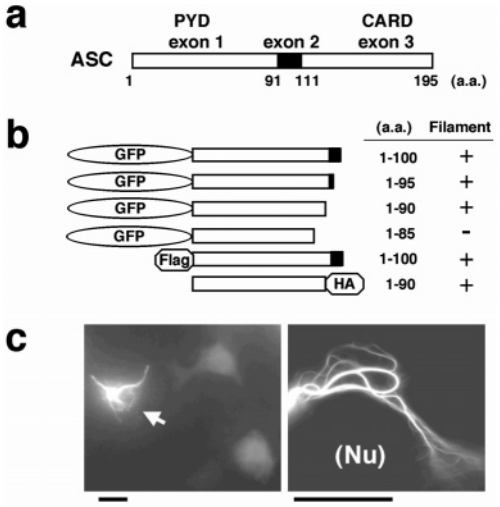

FIGURE 1: PYD filaments. (a) The domain structure of ASC. ASC is encoded by three exons and the PYD resides in exon 1. (b) Filament formation of GFP-tagged and HA-tagged PYD of ASC. ASC deletion mutants lacking the CARD were fused to GFP, Flag, or HA as indicated and expressed in Cos7 cells. Filament formation of GFP-tagged PYD was observed in vivo by fluorescence microscopy. Flag-tagged and HA-tagged PYD filaments were observed by immunostaining after fixation. All filament-positive (+) constructs produced PYD filaments in more than 20% of cells expressing each construct. Filament-negative (−) PYD constructs showed no filamentous structure. (c) Morphology of PYD filaments. GFP-tagged ASC PYD (residues 1−90) was expressed in Cos7 cells and photographed 24 h after transfection of the plasmid. Left panel: example of a living cell producing GFP-tagged PYD filaments (arrow) as seen by fluorescence microscopy. Right panel: photograph at a higher magnification. (Nu): nucleus. Bars: 10 μm.

Table 1: Filament Formation by ASC PYDs Containing Mutations of Charged Residues[a]

mutant	filament	solvent accessibility (%)	mutant	filament	solvent accessibility (%)
R3A	+	69	R41A	−	46
R5A	+	30	R41Q	−	
D6A	+	50	R41K	+	
D10A	+	64	R41W[c]	−	
E13A	+	60	D48A	−	57
E18A	+	68	D48N	−	
E19A	−	39	D48E	−	
E19Q	+		D48R[b]	−	
K21A	−	48	D51A	−	53
K21Q	−		D51N	−	
K21R	+		D51E	+	
K21E[b]	−		D51K[b]	−	
K22A	+	49	K54A	+	49
K24A	+	8	K55A	+	40
K26A	−	28	E62A	−	47
K26Q	−		E62Q	+	
K26R	+		E67A	−	61
R33A	+	82	E67Q	+	
E34A	+	98	R74A	+	69
R38A	+	41	D75A	+	32
			E80A	+	71

[a] GFP-tagged ASC PYD mutants were expressed in Cos7 cells and their filament formations were examined. Positive mutants (+) showed filamentous structures in more than 10% of the fluorescent cells, while negative mutants (−) showed no filamentous structures. The solvent accessibility reports the accessibility of the side chain of the unmutated residue X in the three-dimensional structure of the ASC PYD compared with the solvent accessibility in a helical Gly−X−Gly peptide with a fully extended side chain. [b] This mutation introduces a residue present in the protein pyrin (Figure 3). [c] The corresponding R42W mutation of pyrin is a cause of FMF disease (*31*).

amino acids 1−85 of ASC, all the mutants produced PYD filaments (Figure 1). PYD filaments were observed in more than 10% of cells expressing the GFP-tagged ASC PYD 24 h after transfection. This result demonstrates that the polypeptide comprising amino acids 1−90 is sufficient for the filament formation.

Since GFP (27 kDa) is larger than the ASC PYD (~10 kDa), the large GFP tag could conceivably affect oligomerization of the ASC PYD. Therefore, we also explored the use of two small tags, Flag and HA, instead of GFP. When fused to a N-terminal Flag or a C-terminal HA (Figure 1), both Flag-tagged and HA-tagged ASC PYDs produced filamentous structures 24 h after transfection in more than 20% of the cells expressing them. The morphology of both Flag-tagged and HA-tagged PYD filaments was indistinguishable from that of GFP-tagged PYD filaments. These observations suggested that GFP did not interfere with PYD filament formation. The GFP-tagged ASC PYD (amino acids 1−90) was subsequently used for the point mutation study.

PYD Filaments and Cytoskeletons. The pattern of ASC PYD filaments resembles that of cytoskeletal structures. To examine the relationship of ASC PYD filaments with the cytoskeleton, we immunostained cells expressing ASC PYD with anti-tubulin, anti-actin, or anti-vimentin antibodies. We also used anti-cytokeratin antibodies recognizing cytokeratins 1, 4, 5, 6, 8, 10, 13, 18, and 19. None of these cytoskeletal markers were co-localized with ASC PYD filaments (data not shown). Although we cannot rule out association of ASC PYD filaments with some unknown cytoskeletal component, PYD filament formation seems to be driven by self-association of ASC PYDs rather than association with the cytoskeleton.

Mutations of Charged Residues. On the basis of the pronounced electrostatic dipole moment present in the structure of the ASC PYD and the important role of charged residues played in complexes between DDs and CARDs (*28*, *29*), charged residues are likely to be of great importance also for PYD−PYD interactions (*5*, *18*, *19*, *30*). To verify this prediction, we replaced all the residues with charged side chains in the PYD of human ASC with alanine and examined whether these alanine mutants produced filamentous structures in transfected cells. Filament formation of each mutant was tested at least five times by using various amounts of plasmid DNAs for transfection and the expression levels measured with fluorescence intensity and immunoblotting. Immunoblotting analyses of total cell extracts of the transfected cells showed that all the ASC PYD mutants were expressed at almost the same levels as the wild-type ASC PYD. The mutants E19A, K21A, K26A, R41A, D48A, D51A, E62A, and E67A produced no filamentous structures (Table 1). To assess the importance of a negative charge at these positions, we subsequently generated eight point mutations, where these amino acid residues were substituted with glutamine (Q) or asparagine (N) (Table 1). The mutants E19Q, E62Q, and E67Q were found to produce PYD filaments. Clearly, the charge of these residues is not required for filament formation, suggesting that their mutation to alanine compromised filament formation by disturbing the structure of the domain. In contrast, the mutants K21Q, K26Q, R41Q, D48, and D51N did not show filaments,

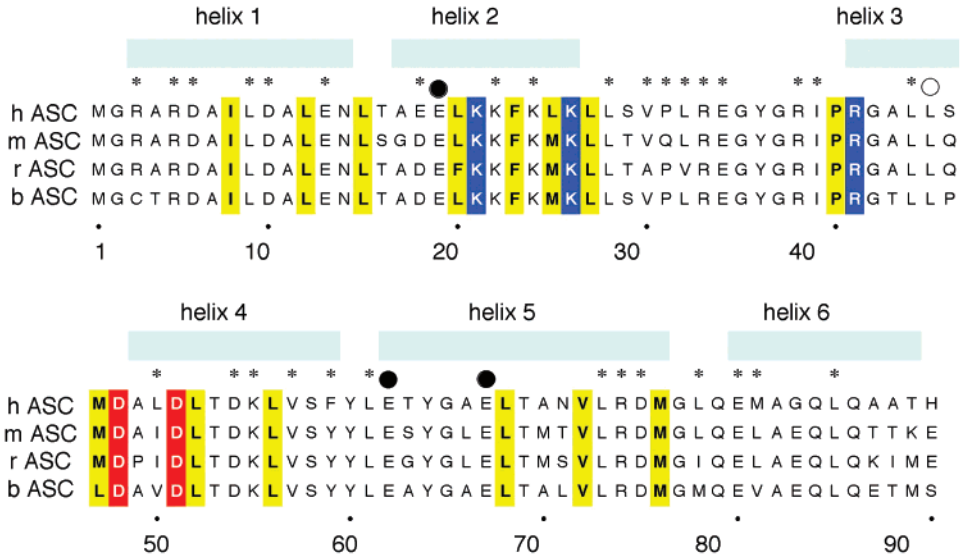

FIGURE 2: Amino acid sequence of ASC PYDs and overview of the present mutation analysis of the human ASC PYD. The PYD sequences of human (h), mouse (m), rat (r), and bovine (b) ASC are aligned. Asterisks identify charged and hydrophobic residues retaining the ability of filament formation upon mutation to alanine. The following colors were used for the amino acid residues where filament formation was prevented by mutation to alanine: blue, positively charged residues; red, negatively charged residues; yellow, hydrophobic residues. Filled circles above the alignment identify glutamic acid residues where the size of the side chain seems to be more important than its charge, as mutation to alanine and glutamine abolishes and retains the capability of filament formation, respectively. An open circle marks L45. Although this residue is solvent-exposed and mutation to alanine suppressed filament formation, it does not seem to be directly involved in intermolecular interactions, since filament formation was retained after mutations to larger residues, including hydrophilic and charged residues (Table 1). Bars at the top mark the helices determined by NMR spectroscopy (*18*).

indicating that the charges provided by the side chains of K21, K26, R41, D48, and D51 play critical roles in PYD filament formation. To confirm this hypothesis, we substituted each charged residue with another amino acid of the same charge. The K21R, K26R, R41K, and D51E mutants produced PYD filaments, highlighting the importance of charge at these positions, whereas the D48E mutant did not. Table 1 and Figure 2 provide a summary of these results. In the case of D48, it appears that both the size and negative charge of its side chain are critical for PYD filament formation in human ASC despite high solvent exposure (Table 1). Interestingly, sequence alignment of human and viral PYD proteins shows that, unlike D51, D48 is never substituted with E in any of the PYDs (Figure 3).

Comparison of the Charged Residues of ASC with Those of Pyrin. Of the five charged residues identified as critical for filament formation in the PYD of ASC, only K26 and R41 are conserved in the PYD of pyrin (Figure 3). To check whether correct charges are sufficient for filament formation, K21, D48, and D51 of ASC were substituted with the charged residues E, R, and K, respectively, present in the PYD of pyrin (Figure 3). As shown in Table 1, the K21E, D48R, and D51K mutants produced no filamentous structures. FMF is caused by point mutations in pyrin. One of these FMF-associated mutations, R42W, is located in the PYD of pyrin (*31*). This residue corresponds to R41 in ASC. R41W mutant of ASC PYD produced no filamentous structures in cells.

Mutations of Hydrophobic Residues. To probe the possible role of hydrophobic interactions in PYD−PYD interactions, all residues with large hydrophobic side chains were replaced by alanine in single point mutations except for the N-terminal methionine. Fifteen mutants (I8A, L12A, L15A, L20A, F23A, L25A, L27, P40, L45A, M47, L52, L56, L68, V72, and M76) of a total of 30 mutants lost the ability to form filamentous structures (Table 1 and Figure 2). Immunoblotting analyses of total cell extracts of the transfected cells confirmed that all the ASC PYD mutants were expressed at almost the same levels as the wild-type ASC PYD (data not shown). Most of the filament-deficient mutants displayed a diffuse cytoplasmic and nuclear distribution.

The NMR structure of the PYD of ASC shows that many of the hydrophobic residues contribute to the hydrophobic core of the three-dimensional structure, displaying very little solvent exposure. Mutations of these residues to alanine are thus likely to prevent filament formation by affecting the three-dimensional structure of the domain. For example, F23 in helix 2 is completely buried in the PYD of ASC (Table 1) and its conservation among PYD proteins (Figure 3) suggests that it is structurally important. Disruption of filament formation observed for the F23A mutant may thus be explained by a disturbed protein structure, whereas the F23L mutant seems to be structurally sufficiently conserved to maintain filament formation (Table 2).

Disruption of filament formation upon mutation to alanine was observed for three hydrophobic residues, which display at least 30% solvent accessibility in the NMR structure of the ASC PYD (L25, P40, L45; Table 2), indicating their potential involvement in PYD−PYD interactions. P40 is spatially close to R41, which is also critical for filament formation (Table 1). P40 is thus likely to be involved in PYD−PYD interactions. L25 and, especially, L45 are only poorly conserved in PYDs (Figure 3). Therefore, additional mutants were made for these two residues to assess their importance in PYD−PYD interactions (Table 2). Hydrophobic mutants (M, I, V, F) of L25 produced filamentous structures. In contrast, filament formation was suppressed after mutation to glycine (G) or hydrophilic residues (Q, N, K, E), indicating that filament formation depends on a large hydrophobic side chain at this site. This pattern would be

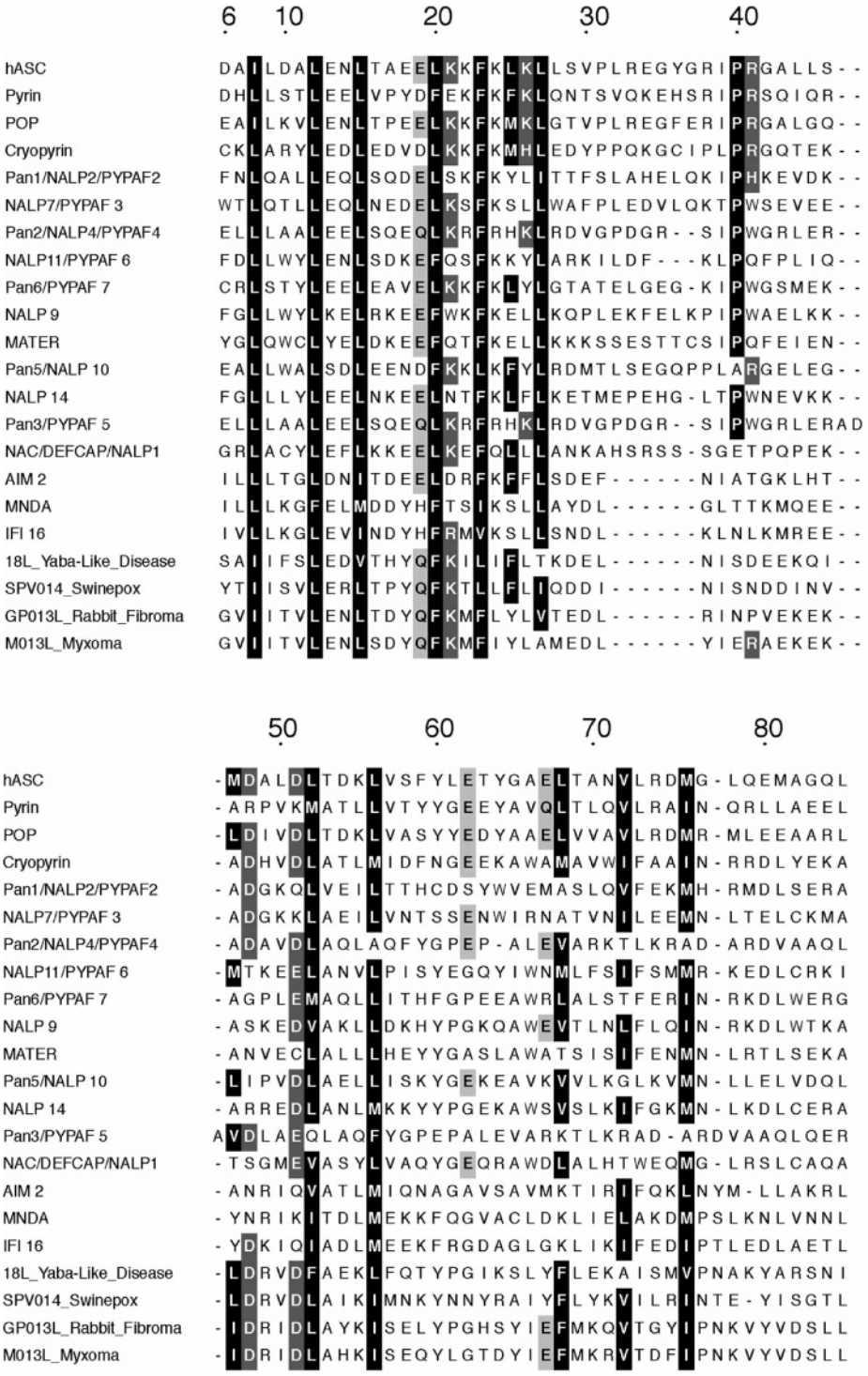

FIGURE 3: Amino acid sequence alignment of PYDs from human and viral proteins. The amino acid sequence data of the PYDs were obtained from the NCBI gene bank (http://www.ncbi.nlm.nih.gov) and previous reports (*10*, *11*, *30*). The alignment highlights the charged and hydrophobic residues found to be critical for PYD filament formation in the present study. White letters with black backgrounds identify nonpolar residues that are identical or similar to hydrophobic residues critical for PYD filament formation. White letters with gray backgrounds identify charged residues that have the same charge as charged residues critical for filament formation in human ASC PYD (K21, K26, R41, D48, and D51). Black letters with gray backgrounds identify glutamic acid (E) and glutamine (Q) residues corresponding to E19, E62, and E67 in human ASC PYD for which the charge is not required for PYD filament formation. The residue numbers of the ASC PYD are shown above the alignment.

expected, if L25 were involved in a hydrophobic intermolecular contact between PYDs. In contrast, hydrophilic and charged mutants (E, Q) of L45 retained the capability of filament formation. Since charged residues are difficult to accommodate in protein−protein interaction surfaces, L45 is probably located outside the PYD−PYD interface. Suppression of filament formation by the L45A mutant may be explained by a structural change induced by the small alanine side chain.

Although M47 is not very solvent accessible in the NMR structure of the ASC PYD, the abolishment of filament formation by the M47A mutation may indicate involvement

Table 2: Filament Formation by ASC PYDs Containing Mutations of Nonpolar Residues[a]

mutant	filament	solvent accessibility (%)	mutant	filament	solvent accessibility (%)
I8A	−	0	L44A	+	0
L9A	+	24	L45A	−	32
L12A	−	0	L45I	+	
L15A	−	2	L45E	+	
L20A	−	16	L45Q	+	
F23A	−	0	M47A	−	7
F23L	+		M47L	+	
L25A	−	45	M47I	+	
L25M	+		M47V	+	
L25I	+		M47Q	−	
L25V	+		M47N	−	
L25F	+		L50A	+	65
L25G	−		L52A	−	1
L25Q	−		L56A	−	0
L25N	−		V57A	+	3
L25K	−		F59A	+	33
L25E	−		L61A	+	57
L27A	−	1	L68A	−	1
L28A	+	38	V72A	−	2
V30A	+	40	L73A	+	0
P31A	+	88	M76A	−	2
L32A	+	9	L78A	+	10
I39A	+	1	M81A	+	16
P40A	−	67	L85A	+	0

[a] GFP-tagged ASC PYD mutants were expressed in Cos7 cells and their filament formations were examined. The criterion for positive filament formation was the same as in Table 1. Side chain solvent accessibilities were also calculated as in Table 1.

of this residue in PYD−PYD interactions, as this residue is replaced by alanine in a large number of other PYDs (Figure 3), apparently without disturbing their structure. Additional mutations of M47 showed that a large hydrophobic side chain at this site is critical for filament formation (Table 2), suggesting that this residue contributes hydrophobic contacts at the PYD−PYD interface.

Localization of Filament-Deficient ASC PYD Mutants in Specks Produced by Full-Length ASC. Overexpression of full-length ASC in cells by transfection with expression plasmids produces large, irregularly distributed structures called "specks" (*1*, *4*, *5*). Since PYD proteins interacting with ASC localize in ASC specks when they are cotransfected with full-length ASC (*1*, *5*, *14*), ASC specks might also play a role under physiological conditions. In contrast to ASC, intracellular expression of pyrin alone results in a diffuse cytoplasmic distribution. However, pyrin localizes in ASC specks when cotransfected with full-length ASC (*5*). To examine whether filament-deficient alanine mutants localize in ASC specks, we coexpressed GFP-tagged ASC PYD mutants with Flag-tagged full-length ASC in Cos7 cells. All filament-deficient ASC PYD mutants of charged and hydrophobic residues were localized in ASC specks (data not shown), indicating the conservation of an intact surface for the interaction with ASC specks. This result suggests that the overall structure of the ASC PYD is still intact after the introduction of point mutations that disturb the structure sufficiently to abolish filament formation.

In vitro Studies of ASC PYD Mutants. To check the degree of structural perturbation introduced by the point mutations in in vitro experiments, His_6-tag constructs were made of the wild-type ASC PYD and a number of selected mutants. The proteins were produced in *E. coli* and purified. The selected mutants comprised the mutants K21A, L25A, R41A, D48A, and D51A, which appear to be involved in intermolecular PYD−PYD interactions according to the filament formation assay. All constructs except D48A expressed protein in high yields. The remaining four proteins were found in the soluble fraction of the cell lysates. In contrast, the wild-type protein was in the insoluble fraction. These data indicated that the mutant proteins were significantly more soluble at neutral pH than the wild-type.

NMR spectra recorded of the purified mutants at pH 7.2 showed the chemical shift dispersion and line widths characteristic of monomeric folded PYD domains (data not shown). The solubility of the mutant D51A was barely sufficient to record a NMR spectrum at neutral pH, but the characteristic spectrum of a folded PYD domain was easily verified at pH 3.7.

DISCUSSION

The data of this study present a comprehensive survey of the roles of different amino acid residues for the self-association of ASC PYDs. Systematic mutation of charged and hydrophobic residues of ASC PYD to alanine revealed that filament formation was abolished by point mutations in 8 of 24 charged residues and 15 of 30 hydrophobic residues. PYD proteins interacting with ASC localize in ASC specks, and this phenomenon has been used as evidence for their specific interactions with ASC (*5*−*7*). We observed, however, that all alanine mutants of ASC PYD concentrated in specks produced by full-length coexpressed ASC, independent of their capability to form filaments. Therefore, we used filament formation as a more sensitive assay of ASC PYD self-association. Disruption of filament formation could be affected in two ways: (i) by mutation of residues located at the protein−protein interface and (ii) indirectly by the structural disruption resulting from mutation of a buried residue. Several measures were taken to ascertain the identification of interfacial residues. First, data from residues with buried side chains were disregarded, unless mutation to alanine could reasonably be expected not to disrupt the three-dimensional fold of the domain, based on the frequent presence of alanine residues at these positions in other PYD-containing proteins. Second, several residues were probed by further mutations to different polar and nonpolar residues to establish the importance of charge or hydrophobicity at the respective sites. Third, a few key mutants of the ASC PYD were expressed with a His-tag, purified, and analyzed by NMR spectroscopy, confirming that their three-dimensional structure was still intact. The residues identified in this way were distributed over coherent surface areas of the three-dimensional ASC PYD structure (Figure 4), lending additional support for their involvement in direct PYD−PYD interactions.

Notably, the NMR structure of the wild-type ASC PYD had to be determined at pH 3.7 from refolded protein (*18*), because the protein precipitated at neutral pH. In contrast, all His-tagged mutants expressed in *E. coli* in high yield in the present study (K21A, L25A, R41A, and D51A) were found in the soluble fraction of the cell lysate at neutral pH. These in vitro results confirm that the mutants are less likely to aggregate compared to the wild-type ASC PYD, strongly

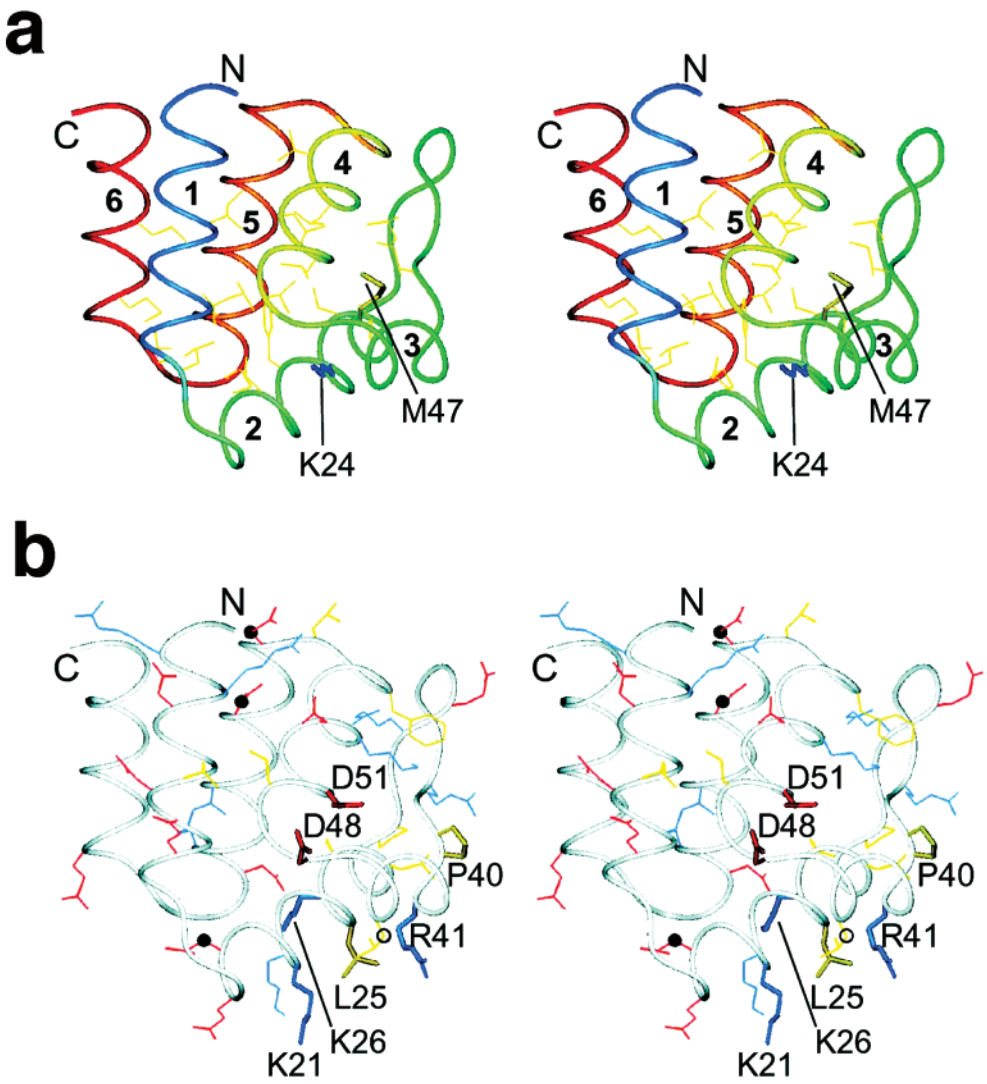

FIGURE 4: Stereoviews of the human ASC PYD, summarizing the mutation results. Side chains are shown only for those residues that were mutated to Ala in the present study. The following colors were used for the amino acid side chains: blue, positively charged side chains (K, R); red, negatively charged side chains (E, D); yellow, hydrophobic side chains (I, L, M, F, P, V). The N- and C-terminal ends of the domain are labeled. (a) View of mutated amino acid side chains with less than 20% average side chain solvent accessibility in the NMR structure. For these residues, mutations may have resulted in loss of function due to structural perturbation of the hydrophobic core. Among the mutated residues, K24 was the only charged residue with less than 20% side chain solvent accessibility. Mutation of M47 resulted in loss of filament formation either because of disruption of the protein structure or because of its location near the putative PYD−PYD interaction surface. The helices are identified with numbers. (b) View of mutated amino acid side chains with more than 20% average side chain solvent accessibility. Side chains that disrupted filament formation upon mutation are labeled with their one-letter amino acid symbol and their sequence number; for the charged residues among these, mutations to Ala as well as loss-of-charge mutations resulted in loss of filament formation. Mutations of unlabeled side chains did not disrupt filament formation. Black spheres identify the side chains of three Glu residues which led to loss of filament formation upon mutation to Ala but not upon mutation to Gln. The charge of these residues thus does not seem critical for PYD−PYD interactions in ASC. Similarly, a circle identifies the side chain of L45, which led to loss of filament formation upon mutation to Ala but not upon mutation to Ile, Gln, or Glu.

suggesting that the filament formation observed in vivo is based on direct PYD−PYD interactions and not mediated by other factors.

Interactions between residues of opposite charge are determinants of homo- and heterophilic interactions between DDs, DEDs, and CARDs (*28*, *29*, *32*, *33*). Our present results provide experimental proof for earlier predictions that charged residues also play a crucial role for the self-association of PYDs (*5*, *18*, *19*, *30*). In particular, the mutation data demonstrate the importance of K21, K26, R41, D48, and D51 for the production of ASC PYD filaments.

On the basis of the PYD structure of ASC, the positively charged side chains of K21, K26, and R41 form a positively charged cluster. Similarly, the negatively charged side chains of D48 and D51 are close together (Figure 4b). These two clusters of opposite charge are separated by the backbone of helix 3. It would thus be plausible that intermolecular electrostatic interactions between the positively charged side chains of K21, K26, and R41 in one molecule and the negatively charged side chains of D48 and D51 in another molecule drive the polymerization and filament formation. As these interactions affect only a relatively small fraction of the surface area of the PYD at the far end of the N- and C-termini, it is not surprising that fusion proteins with GFP and other domains retain the propensity for filament formation.

FMF is caused by point mutations in pyrin. One of these FMF-associated mutations, R42W, is located in the PYD of

pyrin (*31*). This residue corresponds to R41 in ASC. In the context of the ASC PYD, the mutation R41W was found to abolish filament formation. It would be intriguing if the molecular mechanism behind the FMF mutation R42W of pyrin were based on a disrupted interaction between the PYDs from pyrin and ASC. This interaction is known to be of functional importance since pyrin interacts with ASC to inhibit ASC-mediated caspase-1 activation (*5*, *34*, *35*). Notably, however, the sequence conservation between the PYDs from ASC and pyrin is limited. For example, of the five charged residues found to be essential for filament formation of ASC PYD, only two are conserved in pyrin. Furthermore, mutation of the nonconserved residues K21, D48, and D51 in ASC to the oppositely charged residues E, R, and K, respectively, found in pyrin (Figure 3) abolished the formation of filamentous structures (Table 1). Point mutations of ASC are thus not sufficient to simulate the ASC-binding function of pyrin. A more thorough mutational study of the PYD of pyrin will be required to shed light on the role of these oppositely charged residues of pyrin for its inhibitory activity.

The PYD−PYD interactions between residues of opposite charge are supported by hydrophobic interactions. Among the 30 mutants of hydrophobic residues of the ASC PYD, 15 mutants lost the filament-forming activity. Three of these (L25A, P40A, L45A) affected residues for which the side chains are highly solvent exposed in the NMR structure of the domain (Table 2). In particular, L25 and P40 could plausibly be involved in direct PYD−PYD contacts, since mutation of L25 to hydrophilic or charged residues suppressed filament formation and both residues are spatially close to K21, K26, and R41 identified as important for filament formation (see above). In contrast, L45 is less likely to be located in the PYD−PYD interface, as mutation to glutamate and other residues of similar size did not abolish filament formation.

Overall, our results underline the role of helices 2 and 3 in PYD−PYD interactions and suggest that the binding between the ASC PYDs is supported by hydrophic interactions. M47 and, possibly, K24 also form part of this interaction surface. Both residues are barely solvent accessible, yet only the M47A mutation interfered with filament formation (Tables 1 and 2). Although the side chain of M47 contributes to the hydrophobic core of the protein only superficially (Figure 4a), it cannot be ruled out that the M47A mutation affects the structure of the PYD. Notably, however, this residue is substituted by alanine in a large number of naturally occurring PYDs (Figure 3), suggesting that it is not a structurally important residue.

The extent of the present mutational analysis allows us to exclude a role of helix 1 for filament formation. Crystal structures of the complex between the CARD domains of the procaspase-9 prodomain and Apaf-1 and the complex between Pelle and Tube death domains showed that helix 1 was involved in both complexes of these members of the death domain superfamily (*28*, *29*). Our results thus indicate that PYD−PYD interactions of human ASC use a different binding mode. As also helices 2, 3, and 4 are engaged in the interface of the complex between the procaspase-9 prodomain and Apaf-1, and residues from these three helices are also required for filament formation of ASC PYD, it may be tempting to model a PYD−PYD complex based on this structure. Helix 1 is, however, so deeply involved in the prodomain−Apaf-1 interface that very little contact area would be left without it.

I8, L12, L15, L20, F23, L27, L52, L56, L68, V72, and M76 are buried residues, which contribute to the hydrophobic core of the protein (*18*). Their mutations to alanine resulted in loss of PYD filaments presumably due to perturbation of the PYD structure. Most of these 11 hydrophobic core residues are highly conserved among human and viral PYD family proteins (Figure 3), indicative of a conserved structural role.

P42 of the Nalp1 PYD is located in an unstructured polypeptide segment replacing helix 3 in the Nalp1 PYD (*19*). The corresponding residue in ASC PYD (P40) immediately precedes helix 3 (Figure 4). While there is no regular secondary structure in the polypeptide segment between helices 2 and 3 of the ASC PYD, this segment does not show enhanced mobility as in Nalp1 PYD. Figure 3 shows that the presence of a proline residue at position 40 correlates with the presence of a longer linker peptide between helices 2 and 3. Our mutation study shows that P40 but not the linker peptide plays a role in filament formation (Figure 2). It is thus uncertain whether homologous PYD−PYD interactions depend on the presence of a long connecting linker between helices 2 and 3.

While the present study suggests a particular mode of PYD−PYD interactions in ASC, other modes may occur between other members of the PYD family. For example, viral and interferon-inducible PYD proteins (IFI16, AIM2, and MNDA) do not have the critical proline residue at position 40 and may thus engage in different protein−protein interactions. PYDs also have the capability of binding to non-PYD proteins, as demonstrated by the ASC PYD-Bax interaction (*36*). Considering the structural similarity between proteins of the death domain family of proteins and the documented variability of their intermolecular associations (*37*), the structure of a complex between PYDs presents an intriguing question. The present data provide the basis for the construction of a homodimeric complex between ASC PYDs, which will yield more detailed insight into PYD−PYD interactions.

ACKNOWLEDGMENT

We thank Dr. J. C. Reed (Burnham Institute) for critical reading of this manuscript, Dr. J. Masumoto for the preparation of expression plasmids, and T. Shijo for preliminary mutation experiments. Access to the Biomolecular Resource and NMR facilities at the Australian National University is gratefully acknowledged.

REFERENCES

1. Masumoto, J., Taniguchi, S., Ayukawa, K., Sarvotham, H., Kishino, T., Niikawa, N., Hidaka, E., Katsuyama, T., Higuchi, T., and Sagara, J. (1999) ASC, a novel 22-kDa protein, aggregates during apoptosis of human promyelocytic leukemia HL-60 cells, *J. Biol. Chem. 274*, 33835−33838.
2. Conway, K. E., McConnell, B. B., Bowring, C. E., Donald, C. D., Warren, S. T., and Vertino, P. M. (2000) TMS1, a novel proapoptotic caspase recruitment domain protein, is a target of methylation-induced gene silencing in human breast cancers, *Cancer Res. 60*, 6236−6242.
3. McConnell, B. B., and Vertino, P. M. (2000) Activation of a caspase-9-mediated apoptotic pathway by subcellular redistribution

of the novel caspase recruitment domain protein TMS1, *Cancer Res. 60*, 6243−6247.
4. Masumoto, J., Taniguchi, S., and Sagara, J. (2001) Pyrin N-terminal homology domain- and caspase recruitment domain-dependent oligomerization of ASC, *Biochem. Biophys. Res. Commun. 280*, 652−655.
5. Richards, N., Schaner, P., Diaz, A., Stuckey, J., Shelden, E., and Wadhwat, A., and Gumucio, D. L. (2001) Interaction between pyrin and the apoptotic speck protein (ASC) modulates ASC-induced apoptosis, *J. Biol. Chem. 276*, 39320−39329.
6. Stehlik, C., Fiorentino, L., Dorfleutner, A., Bruey, J., Ariza, M., Sagara, J., and Reed J. C. (2002) The PAAD/PYRIN-family protein ASC is a dual regulator of a conserved step in nuclear factor kappaB activation pathways, *J. Exp. Med. 196*, 1605−1615.
7. Manji, G., Wang, L., Geddes, B. J., Brown, M., Merriam, S., Al-Garawi, A., Mak, S., Lora, J. M., Briskin, M., Jurman, M., Cao, J., DiStefano, P. S., and Bertin, J. (2002) PYPAF1, a PYRIN-containing Apaf1-like protein that assembles with ASC and regulates activation of NF-kappa B, *J. Biol. Chem. 277*, 115701−11575.
8. Fairbrother, W. J., Gordon, N. C., Humke, E. W., O'Rourke, K. M., Starovasnik, M. A., Yin, J. P., and Dixit, V. M. (2001) The PYRIN domain: a member of the death domain-fold superfamily, *Protein Sci. 10*, 1911−1918.
9. Bertin, J., and DiStefano, P. S. (2000) The PYRIN domain: a novel motif found in apoptosis and inflammation proteins, *Cell Death Differ. 7*, 1273−1274.
10. Pawlowski, K., Pio, F., Chu, Z., Reed, J. C., and Godzik, A. (2001) PAAD − a new protein domain associated with apoptosis, cancer and autoimmune diseases, *Trends Biochem. Sci. 26*, 85−87.
11. Staub, E., Dahl, E., and Rosenthal, A. (2001) The DAPIN family: a novel domain links apoptotic and interferon response proteins, *Trends Biochem. Sci. 26*, 83−85.
12. Martinon, F., Burns, K., and Tschopp, J. (2002) The inflammasome: a molecular platform triggering activation of inflammatory caspases and processing of proIL-beta, *Mol. Cell 10*, 417−426.
13. Srinivasula, S. M., Poyet, J. L., Razmara, M., Datta, P., Zhang, Z., and Alnemri, E. S. (2002) The PYRIN−CARD protein ASC is an activating adaptor for caspase-1, *J. Biol. Chem. 277*, 21119−21122.
14. Stehlik, C., Lee, S. H., Dorfleutner, A., Stassinopoulos, A., Sagara, J., and Reed, J. C. (2003) Apoptosis-associated speck-like protein containing a caspase recruitment domain is a regulator of procaspase-1 activation, *J. Immunol. 171*, 6154−6163.
15. Mariathasan, S., Newton, K., Monack, D. M., Vucic, D., French, D. M., Lee, W. P., Roose-Girma, M., Erickson, S., and Dixit, V. M. (2004) Differential activation of the inflammasome by caspase-1 adaptors ASC and Ipaf, *Nature 430*, 213−218.
16. Salvesen, G. S., and Dixit, V. M. (1999) Caspase activation: the induced-proximity model, *Proc. Natl. Acad. Sci., U.S.A. 96*, 10964−10967.
17. Kumar, S., and Colussi, P. A. (1999) Prodomains−adaptors−oligomerization: the pursuit of caspase activation in apoptosis, *Trends Biochem. Sci. 24*, 1−4.
18. Liepinish, E., Barbals, R., Dahl, E., Sharipo, A., Staub, E., and Otting, G. (2003) The death-domain fold of the ASC PYRIN domain, presenting a basis for PYRIN/PYRIN recognition, *J. Mol. Biol. 332*, 1155−1163.
19. Hiller, S., Kohl, A., Fiorito, F., Herrmann, T., Wider, G., Tschopp, J., Grütter, M. G., and Wüthrich, K. (2003) NMR structure of the apoptosis- and inflammation-related NALP1 pyrin domain, *Structure 11*, 1199−1205.
20. Siegel, R. M., Martin, D. A., Zheng, L., Ng, S., Bertin, J., Cohen, J., and Lenardo, M. J. (1998) Death-effector filaments: novel cytoplasmic structures that recruit caspases and trigger apoptosis, *J. Cell Biol. 141*, 1243−1253.
21. Perez, D., and White, E. (1998) E1B 19K inhibits Fas-mediated apoptosis through FADD-dependent sequestration of FLICE, *J. Cell Biol. 141*, 1255−1266.
22. Yan, M., Lee, J., Schilbach, S., Godard, A., and Dexit, V. (1999) mE10, a novel caspase recruitment domain-containing pro-apoptotic molecule, *J. Biol. Chem. 274*, 10287−10292.
23. Guiet, C., and Vito, P. (2000) Caspase recruitment domain (CARD)-dependent cytoplasmic filaments mediate bcl10-induced NF-kappaB activation, *J. Cell. Biol. 148*, 1131−1139.
24. Imai, Y., Matsushima, Y., Sugimura, T., and Terada, M. (1991) A simple and rapid method for generating a deletion by PCR, *Nucleic Acids Res. 19*, 2785.
25. Neylon, C., Brown, S. E., Kralicek, A. V., Miles, C. S., Love, C. A., and Dixon, N. E. (2000) Interaction of the *Escherichia coli* replication terminator protein (Tus) with DNA: a model derived from DNA-binding studies of mutant proteins by surface plasmon resonance, *Biochemistry 39*, 11989−11999.
26. Studier, F. W., Rosenberg, A. H., Dunn, J. J., and Dubendorff, J. W. (1990) Use of T7 RNA polymerase to direct expression of cloned genes, *Methods Enzymol. 185*, 60−89.
27. Sevilla-Sierra, P., Otting, G., and Wüthrich, K. (1994) Determination of the nuclear magnetic resonance structure of the DNA-binding domain of the P22 c2 repressor (1−76) in solution and comparison with the DNA-binding domain of the 434 repressor, *J. Mol. Biol. 235*, 1003−1020.
28. Xiao, T., Towb, P., Wasserman, S. A., and Sprang, S. R. (1999) Three-dimensional structure of a complex between the death domains of Pelle and Tube, *Cell 99*, 545−555.
29. Qin, H., Srinivasula, S. M., Wu, G., Fernandes-Alnemri, T., Alnemri, E. S., and Shi, Y. (1999) Structural basis of procaspase-9 recruitment by the apoptotic protease-activating factor 1, *Nature 399*, 549−557.
30. Liu, T., Rojas, A., Ye, Y., and Godzik, A. (2003) Homology modeling provides insights into the binding mode of the PAAD/DAPIN/pyrin domain, a fourth member of the CARD/DD/DED domain family, *Protein Sci. 12*, 1872−1881.
31. Hull, K. M., Shoham, N., Chae, J. J., Aksentijevich, I., and Kastner, D. L. (2003) The expanding spectrum of systemic autoinflammatory disorders and their rheumatic manifestations, *Curr. Opin. Rheumatol. 15*, 61−69.
32. Chou, J. J., Matsuo, H., Duan, H., and Wagner, G. (1998) Solution structure of the RAIDD CARD and model for CARD/CARD interaction in caspase-2 and caspase-9 recruitment, *Cell 94*, 171−180.
33. Eberstadt, M., Huang, B., Chen, Z., Meadows, R. P., Ng, S., Zheng, L., Lenardo, M. J., and Fesik, S. W. (1998) NMR structure and mutagenesis of the FADD (Mort1) death-effector domain. Solution structure of the RAIDD CARD and model for CARD/CARD interaction in caspase-2 and caspase-9 recruitment, *Nature 392*, 941−945.
34. Chae, J. J., Komarow, H. D., Cheng, J., Wood, G., Raben, N., Liu, P. P., and Kastner, D. L. (2003) Targeted disruption of pyrin, the FMF protein, causes heightened sensitivity to endotoxin and a defect in macrophage apoptosis, *Mol. Cell 11*, 591−604.
35. Dowds, T. A., Masumoto, J., Chen, F. F., Ogura, Y., Inohara, N., and Nunez, G. (2003) Regulation of cryopyrin/Pypaf1 signaling by pyrin, the familial Mediterranean fever gene product, *Biochem. Biophys. Res. Commun. 302*, 575−580.
36. Ohtsuka, T., Ryu, H., Minamishima, Y. A., Macip, S., Sagara, J., Nakayama, K. I., Aaronson, S. A., and Lee, S. W. (2004) ASC is a Bax adaptor and regulates the p53-Bax mitochondrial apoptosis, *Nat. Cell Biol. 6*, 121−128.
37. McConnell, B. B., and Vertino, P. M. (2004) TMS1/ASC: the cancer connection, *Apoptosis 9*, 5−18.

BI048374I